Acta Cryst. (1976). A32, 529

Investigation of the Bonding Mechanism in Pyrite using the Mössbauer Effect and X-ray Crystallography

BY SAMUEL L. FINKLEA III AND LECONTE CATHEY

Department of Physics and Astronomy, University of South Carolina, Columbia, South Carolina 29208, *U.S.A.*

AND E. L. AMMA

Department of Chemistry, University of South Carolina, Columbia, South Carolina 29208, *U.S.A.*

(*Received* 28 *July* 1975; *accepted* 23 *December* 1975)

The nature of the bonding in pyrite is considered in relation to the origin of the quadrupole splitting observed by means of the Mössbauer effect and the angular variation of the recoil-free fraction. It is found that neither crystal-field effects nor non-stoichiometry are enough to account for the observed splitting. Consideration of molecular orbital effects, however, shows that a very small amount of electron delocalization is enough to cause the observed splitting because of the strong effects the valence electrons have on the iron nucleus. It is also found that, contrary to previously published data, the recoil-free fraction is practically independent of angle. This result is derived from both Mössbauer resonance measurements and an X-ray structure determination. The structure determination confirms earlier reports of interatomic distances and angles and also determines the anisotropic thermal parameters for both Fe and S atoms in naturally occurring pyrite. The temperature variation of the isomer shift is measured and interpreted to mean that vibrational modes corresponding to Raman modes are not excited in the pyrite lattice between 10 and 300 K. This complements published IR spectra which show no such modes between 190 and 660 cm^{-1} (equivalent to 274 and 950 K). The isomer shift of pyrite is found to be $0{\cdot}074 \pm 0{\cdot}001$ mm/s relative to Fe in Cu (source and absorber at room temperature) and the quadrupole splitting is $0{\cdot}634 \pm 0{\cdot}006$ mm/s at room temperature. The ratio of intensities of the $\frac{3}{2} \rightarrow \frac{1}{2}$ and $\frac{1}{2} \rightarrow \frac{1}{2}$ transitions of the Mössbauer spectra was typically $1{\cdot}004 \pm 0{\cdot}011$.

I. Introduction

The Mössbauer spectra of Fe^{2+}, Fe^{3+} surrounded by six S atoms has been extensively investigated (Golding & Whitfield, 1966; Frank & Abeledo, 1966; Vainstein, Valov, Larimov & Shullman, 1966; Richards, Johnson & Hill, 1968; Epstein & Straub, 1969; Merrithew & Rasmussen, 1972). In addition, the Mössbauer spectra of a number of Fe–S clusters have been examined because of the relevance of these compounds to Fe–S covalent bonds as well as the relationship of these clusters to biological systems (Averill, Herskovitz, Holm & Ibers, 1973; Bernal, Davis, Good & Chandra, 1972; Balch, 1969).

Iron pyrite has been examined several times by means of the Mössbauer effect (Imbert, Gerard & Wintenberger, 1963; Goodman, 1966; Suzdalev, Vinogradov & Imshennik, 1972; Garg, Lui & Puri, 1974). The spectra reported by these authors show significant differences in the intensity ratios of the two transitions of the Mössbauer spectra. In addition, a preliminary examination of the Mössbauer effect spectrum of pyrite showed that several of the results mentioned above could not be duplicated.

Iron pyrite contains Fe^{2+} low spin, as shown by paramagnetic susceptibility measurements (Serres, 1953). There are no unpaired spins and hence no unpaired electrons around the Fe atoms. The observed electric field gradient (EFG) must therefore arise from some other mechanism. Possible causes include a low site symmetry for the Fe atoms or an anisotropic mean squared displacement of the Fe atoms.

The Fe site symmetry given by the space group *Pa*3, assigned to pyrite by Parker & Whitehouse (1932), is $\bar{3}(S_6)$. Such a high symmetry does not suggest the possibility of a non-zero EFG. However, the anisotropic mean squared displacement of the Fe atoms reported by Suzdalev *et al.* (1972) could explain the observed EFG. Since previous structural determinations of pyrite (Parker & Whitehouse, 1932; Brostigen & Kjekshus, 1969) did not include anisotropic thermal parameters, it was decided to redetermine the structure and include this refinement.

The results of the Mössbauer effect measurements and the crystallographic structure determination are practically identical: the magnitude of principal axes of the mean squared displacement of the Fe atoms in pyrite differ by no more than 9%. This is to be compared with the results of Suzdalev *et al.*, who find that the difference in the magnitude of the principal axes is much larger, about a factor of two.

II. Experimental Mössbauer spectroscopy details

Naturally occurring pyrite from two different sources was used in this experiment. Large, single crystals were purchased from Ward's Natural Science Establishment, Rochester, N.Y. The crystals are stated to be from Ambasaguas, Spain.

X-ray crystallography requires much smaller crystals

than those required for the single-crystal Mössbauer resonance experiment. There were no crystals among those purchased from Ward's, small enough for the X-ray work. Pyrite exhibits conchoidal fractures when struck, rather than cleaving along crystal planes, and as a result it was not possible to obtain suitable small crystals by cleaving one of the same crystals that were used for the Mössbauer resonance experiment. However, crystals suitable for crystallography were obtained from the tailings of a kyanite mine near York, S.C.

Natural pyrite is known to be non-stoichiometric. Natural samples are FeS_n, with n ranging from 1·93 to 2·01 (Smith, 1942). To check the possibility that the pyrite samples used here, being from different locations, might have different stoichiometries, we sent samples of both to a commercial quantitative analytical laboratory. The results of the analysis (Cogswell, 1975) are shown in Table 1.

The amount of Fe was determined by atomic absorption after digestion with HCl and HNO_3. The symbol n is the number of S atoms per Fe atom, as above.

Table 1. *Chemical analysis of natural pyrite samples*

Samples	Fe: % by weight	n
York	45·9	2·05
Ambasaguas	46·9	2·01

While the value of n is slightly larger than those previously reported, the point of interest is that n differs by no more than 2% from the York samples to the Ambasaguas samples. We therefore conclude that, on the basis of this result and the calculation of the EFG due to any non-stoichiometry discussed in §IV(*b*), any differences between the two types of samples are not significant.

It should also be noted that Mössbauer resonance spectra of powder samples from both sources were taken. The spectra are identical, showing no variations in any of the parameters including the temperature dependence of the isomer shift. This indicates that we are justified in using samples from different sources.

To ensure that the samples were true single crystals, Laue photographs of the Mössbauer samples were obtained. No evidence of twinning was observed in any of the samples selected for study here.

Only naturally occurring pyrite was used in this work. Powder samples from both sources were prepared by grinding fragments with a mortar and pestle. The powder was then imbedded in paraffin on household aluminum foil, which completed the sample preparation. Single-crystal slices were cut from one single crystal and mounted on 0·006″ (0·152 mm) thick microscope-slide cover glasses using Hilquest epoxy. The slices were hand lapped using carborundum powder on plate glass until the edges of the crystal began to feather. The thickness of the finished samples ranged from 0·0021″ to 0·0035″ (0·053 mm to 0·089 mm).

The source was commercially prepared ^{57}Fe in Cu. The spectometer was operated in transmission geometry and in the constant acceleration mode. Velocity calibration was determined by using standard reference materials [Fe in Fe and $Na_2Fe(CN)_5NO.2H_2O$].

Data reduction was done by least-squares fitting of Lorentzians to the experimental data. The method of fitting follows the modified Gauss–Newton method (Chrisman & Tumolillo, 1969). Backgrounds are flat and all parameters were varied in the fitting routines. A typical spectrum is shown in Fig. 1.

III. Crystallographic structure solution

The pyrite used in the structure determination was found in the tailings of the Commercial ore kyanite mine near York, S.C. Pyrite crystals were found in abundance mixed in sand. Small, well formed rectangular prisms with no visual signs of twinning were examined and oscillation and Weissenberg photographs were used to reject any of the remainder which were twinned. Weissenberg data *hk*0, *hk*1, and *hk*2 showed the crystals to be cubic with systematic absences 0*kl*, *k* odd; *h*0*l*, *l* odd; *hk*0 *h* odd, confirming the space group as *Pa*3.

Two single crystals: 0·097 × 0·092 × 0·152 and 0·171 × 0·027 × 0·0135 mm were mounted with the long directions approximately parallel to the φ axis on a Picker diffractometer and aligned by variations of well known techniques (Furnas, 1957; Busing & Levy, 1967; Knox, 1967). A locally written least-squares fit program of the χ, φ, and 2θ angles of 15 reflections accurately centered on the diffractometer was used to determine the lattice constants at 23–25 °C (λ=0·71068 Å for Mo $K\alpha$): a= 5·4281 ± 0·0001 Å. With Z=4 the calculated density is 5·06 g cm^{-3}, and the observed density is between 4·951 (Anderson, 1937) and 5·020 g cm^{-3} (Smith, 1942). The linear absorption coefficient μ was calculated to be

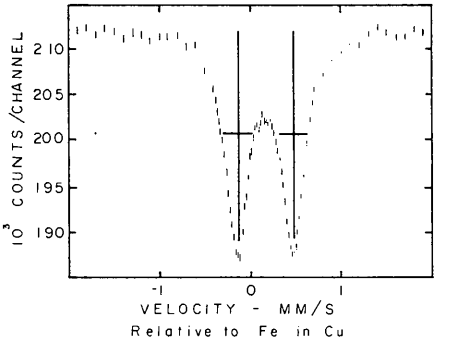

Fig. 1. Mössbauer spectrum of pyrite. The crystal orientation is parallel to the [010] axis. The temperature is 100 K. The small vertical bars denote $\pm\sqrt{N}$ where N is the number of counts per channel. The crosses indicate the least-squares fitted energies, intensities, and linewidths of the two transitions.

116·4 cm^{-1} with Mo $K\alpha$ radiation. With this μ and the above crystal dimensions the maximum and minimum transmission coefficients for a crystal bound by the (100), ($\bar{1}$00), (010), (0$\bar{1}$0), (001) and (00$\bar{1}$) planes were 0·457 and 0·334, respectively (Hamilton, 1964). Lorentz–polarization corrections were made and the intensities reduced to structure factors.*

A total of 456 reflections from one data set and 500 reflections from another crystal in a second set were taken using θ–2θ scan techniques and unfiltered Mo $K\alpha$ radiation. The use of unfiltered radiation was justified by careful examination of the shape of strong reflections which showed that overlap of Mo $K\alpha$ reflections was negligible. For a more complete discussion of the validity of this approach see Young (1965), (Gash, Rodesiler & Amma, 1974).

Data was collected at room temperature for 95·8 s at 0·024°/s and background counts were made for 20·0 s (B_1 and B_2). Reflections were considered absent if the integrated intensity was less than $2{\cdot}0[(2{\cdot}4)^2(B_1+B_2)]^{1/2}$. After removal of redundancies, symmetry-related reflections, and unobserved reflections, a total of 324 reflections remained.

Two crystals and two data sets were used because the diffractometer malfunctioned during data collection and the crystals were lost during the subsequent readjustments.

To check instrumental stability, a standard reflection (511) was measured every 10 reflections. The intensity of the standard was used to normalize the data. Large deviations of the standard were grounds for rejecting the data and resetting the diffractometer.

The take-off angle was 3·7°. The source-to-crystal and crystal-to-counter distances were 18 and 23 cm, respectively. The aperture at the counter was 6 × 8 mm. Plots of measured intensity *vs* 2θ showed that the diffractometer was scanning over the entire reflected peak.

The two data sets were brought to the same relative structure factors by multiplying one set of structure factors by the ratio of the structure factors of the standard reflections for both sets. The atomic scattering factors were taken from Cromer & Waber (1965) and the anomalous dispersion correction from Cromer (1965). The symmetry of space group $Pa3$ requires that one atom lie at the origin and the others at the positions $\pm(uuu)$. Levy (1956) has shown that this places the following constraints on the anisotropic thermal parameters β_{ij} of both sites:

$$\begin{aligned}\beta_{11}&=\beta_{22}=\beta_{33}\\ \beta_{12}&=\beta_{23}=\beta_{13}\,.\end{aligned}\qquad(1)$$

* A list of structure factors has been deposited with the British Library Lending Division as Supplementary Publication No. SUP 31622 (5 pp.). Copies may be obtained through The Executive Secretary, International Union of Crystallography, 13 White Friars, Chester CH1 1NZ, England.

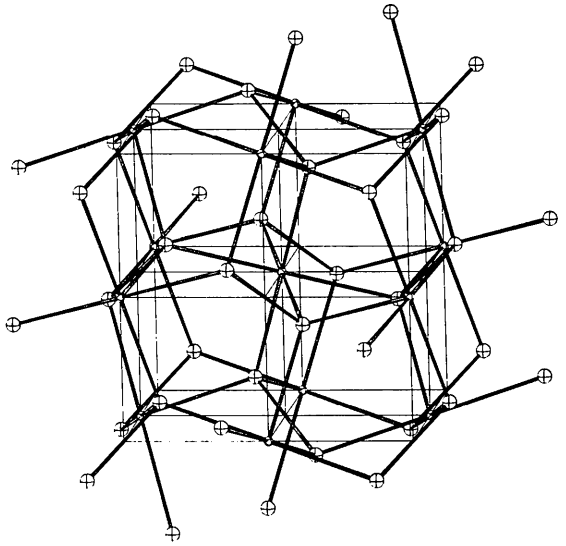

(*a*)

Fig. 2. Pyrite structure. Fe atoms are denoted by small ellipses, the S atoms by large ellipses. The crystal axes are shown as single lines. The diagrams are drawn by *ORTEP* (Johnson, 1965). (*a*) Structural arrangement of pyrite.

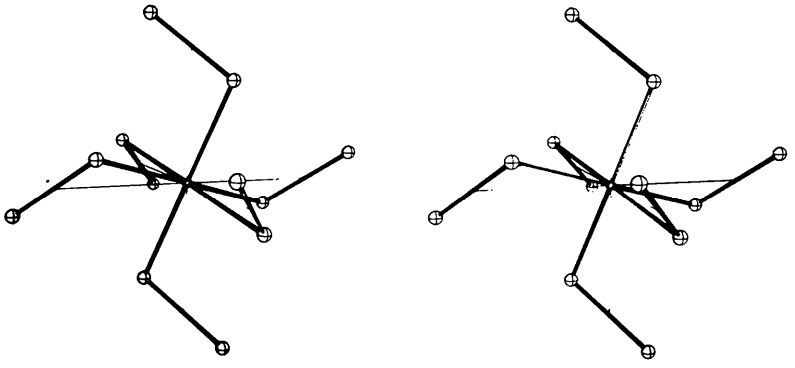

(*b*)

Fig. 2 (*cont.*) (*b*) Stereoscopic view of Fe atom and nearest and next nearest neighbors.

Several cycles of full-matrix least-squares refinement (Busing, Martin & Levy, 1962) with anisotropic thermal parameters brought the residual index R for data set 1 alone to 0·0205 including negatives and 0·0362 for sets 1 and 2 together. The fitted parameters are shown in Table 2 for both fits. The positions and angles are given in Table 3 and the structure is shown in Fig. 2.

Table 2. *Least-squares parameters from crystallographic data*

		Data set 1	Data sets 1 and 2
Fe	multiplicity	0·500	0·500
	position	0·000	0·000
	thermal parameters		
	β_{11}	0·00211 ± 0·00008	0·00211 ± 0·00012
	β_{12}	0·00001 ± 0·00004	−0·00003 ± 0·00011
S	multiplicity	1·000	1·000
	position (u,u,u)	0·38504 ± 0·00005	0·38506 ± 0·00092
	thermal parameters		
	β_{11}	0·00252 ± 0·00008	0·00256 ± 0·00012
	β_{12}	−0·00001 ± 0·00005	0·00004 ± 0·00015

Table 3. *Derived parameters from least-squares parameters*

Solution of data sets 1 and 2
Root-mean-squared displacements (Å)

Fe	0·0554 ± 0·0004	S	0·061 ± 0·014
	0·0554 ± 0·0004		0·061 ± 0·014
	0·0585 ± 0·0016		0·063 ± 0·003

Distances (Å)

Fe–S	2·259 ± 0·005	S–S	2·153 ± 0·006

Angles (°)

S–Fe–S	85·66 ± 0·09, 94·34 ± 0·06
Fe–S–Fe	115·5 ± 0·1
S–S–Fe	102·4 ± 0·2

The good agreement between the results of the two fits seems to indicate that we are justified in combining the data sets.

The Fe atoms are surrounded by six S atoms at 2·259 (5) Å in a distorted octahedral array $(\bar{3},S_6)$. The S–Fe–S angles are 85·66 (9)° compared to the ideal 90°, Fig. 2(*a*) and (*b*). This distortion corresponds to a compression along the [111] crystallographic direction. The next nearest S atom neighbors are those at 3·439 (5) Å which are the set of S atoms bound by covalent bonds to the nearest six S atoms of Fe. The crystallographic symmetry demands that this octahedron is also distorted by exactly the same amount in the same way as is the smallest FeS_6 octahedron. These two octahedra are related by the difference in the Fe–S distance (above) and a rotation of 37·7°.

Each S atom has one nearest neighbor S atom and three nearest neighbor Fe atoms. The site symmetry, $\bar{3}(S_6)$, is that of a distorted tetrahedron. The S–S distance of 2·153 (6) Å is shorter than the Fe–S distances of 2·259 (5) Å and the angles are not the ideal tetrahedral value of 109°. This S–S distance is somewhat on the long side of those reported in a recent compilation of S–S bonded systems (2·00–2·08 Å) (Rodesiler & Amma, 1971).

In space group $Pa3$ the Miller indices h, k and l are not generally permutable. As a consequence of the fact that the general positions (xyz) are not occupied in pyrite, the hkl and khl reflections are equivalent for even–even–even and odd–odd–odd indices. To check for any deviations from cubic symmetry and/or deviations from the requirements of the special positions of $Pa3$, 31 such pairs of equivalent reflections in the data set were examined. The data shown in Table 4 indicate that no such deviations could be detected. The differences between pairs of F(obs) appear uniformly distributed about zero. The null hypothesis that the differences between the odds and evens are not due to chance is rejected between the 50 and 75% levels of confidence by constructing a contingency table (Smith, 1975). The observed distribution about zero of odds and evens may be exceeded by chance at least 43 and 74% of the time, respectively. Hence, we can conclude that the observed differences between equivalent reflections are due entirely to chance. There is no evidence for any departure from cubic symmetry nor from the special constraints of $Pa3$.

Table 4. *F(obs) for equivalent pairs of reflections*

Equivalent pairs are even–even–even or odd–odd–odd. The permutations are $hkl \rightarrow khl$ or $hkl \rightarrow hlk$.

Equivalent reflections	F(obs)	Equivalent reflections	F(obs)
2 4 0	191·3	4 0 6	199·9
2 0 4	184·9	0 4 6	194·6
0 2 6	147·9	1 3 7	149·5
2 0 6	147·2	3 1 7	151·3
1 5 7	140·7	1 5 3	91·2
5 1 7	140·0	5 1 3	91·2
2 4 6	136·0	8 2 0	134·8
4 2 6	135·8	8 0 2	136·4
8 4 2	93·9	7 5 3	85·5
8 2 4	93·6	7 3 5	84·3
6 8 0	63·9	−8 6 2	93·1
8 6 0	63·6	−6 8 2	90·7
10 2 0	158·4	12 2 0	115·1
2 10 0	159·9	2 12 0	111·0
10 4 0	62·4	12 4 0	178·5
4 10 0	59·4	4 12 0	167·4
9 3 1	217·4	11 3 1	126·5
3 9 1	221·8	3 11 1	126·6
9 5 1	228·9	11 5 1	116·1
5 9 1	231·1	5 11 1	115·9
9 7 1	99·7	11 7 1	104·4
7 9 1	99·7	7 11 1	105·4
10 4 2	126·2	12 4 2	110·1
4 10 2	129·9	4 12 2	108·5
10 6 2	119·6	10 8 2	106·9
6 10 2	112·6	8 10 2	109·2
9 5 3	64·9	11 5 3	123·1
5 9 3	71·7	5 11 3	123·6
8 6 4	164·8	10 6 4	135·4
6 8 4	174·5	6 10 4	127·9
9 7 5	146·0		
7 9 5	141·7		

IV. Mössbauer effect measurements

(*a*) *Energy levels and spin state*

Fe^{2+} has a valence electron configuration of $3d^6$. Since the symmetry of the Fe site is that of a trigonally distorted octahedron, the electronic energy levels are split as shown in Fig. 3. Since the paramagnetic susceptibility of pyrite is known to be due entirely to naturally occurring trace impurities, the six valence electrons must occupy the three lowest energy levels to give rise to a net spin of zero (Serres, 1953). As a result, there are no unpaired electrons and any EFG at the Fe nucleus must be due to some other mechanism.

(*b*) *Lattice contributions*

The separation of the E and A_1 states for $I=\frac{3}{2}$ is (Goldanskii & Herber, 1968):

$$\Delta E=\tfrac{1}{2}e^2qQ(1+\eta^2/3)^{1/2} \qquad (2)$$

where

$$\begin{aligned} eq&=eV_{zz}\,,\\ V_{zz}&=\text{major component of EFG}\,,\\ Q&=\text{quadrupole moment}\,,\\ \eta&=\text{asymmetry parameter}\,. \end{aligned} \qquad (3)$$

It is possible to split q into two contributions, lattice and valence:

$$q=(1-\gamma_\infty)q_{\rm lat}+(1-R)q_{\rm val}\,. \qquad (4)$$

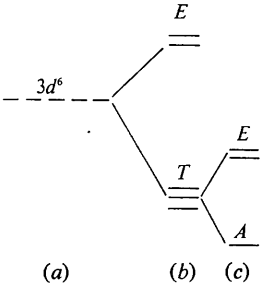

Fig. 3. Splitting of iron valence electron energy levels in lattice sites. (*a*) Free ion energy levels. (*b*) Splitting due to octahedral symmetry (no mixing of E and T levels). (*c*) Splitting due to trigonal distortion of octahedral symmetry.

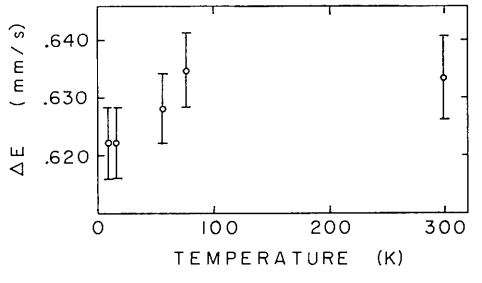

Fig. 4. Temperature dependence of quadrupole splitting of pyrite.

R and γ_∞ are the Sternheimer antishielding factors (Sternheimer & Foley, 1956). The EFG at the nucleus depends on the field gradient due to the external charges and the s electron density at the nucleus. R accounts for the polarization of the core electrons and the consequent changes in s electron density by the valence electrons, and γ_∞ accounts for the polarization of the core by the external charges.

We now consider the evaluation of $q_{\rm lat}$. The electric potential at a field point near the center of an array of N charges is

$$V=\sum_i^N z_ie/|\mathbf{R}_i-\mathbf{r}| \qquad (5)$$

where z_i is the ith charge, $\mathbf{R}_i$ is the vector from the origin to the ith charge, and $\mathbf{r}$ is the vector from the origin to the field point. Then

$$V_{zz}=\lim_{z\to 0}\frac{\partial^2 V}{\partial z^2} \qquad (6)$$

$$=\sum_i^N\frac{z_ie}{R_i^3}(3\cos^2\theta_i-1)\,. \qquad (7)$$

Likewise

$$\eta=\frac{V_{xx}-V_{yy}}{V_{zz}}=\frac{1}{V_{zz}}\sum_i^N\frac{ez_i}{R_i^3}3\sin^2\theta\cos\theta 2\varphi\,, \qquad (8)$$

θ and φ are the usual polar angles.

V_{zz} and η were calculated for the Fe site (0,0,0) in pyrite using (7) and (8). The calculations were done in a new coordinate system $x'y'z'$ defined so that

$$\begin{aligned} x'&=(1/\sqrt{2})\,(x\ -y\ 0)\\ z'&=(1/\sqrt{3})\,(x\ y\ z)\\ y'&=z'\times x'. \end{aligned} \qquad (9)$$

This choice of axes puts V_{zz} along the threefold axis of the smaller octahedron surrounding the Fe atom.

To ensure convergence of the sum, atoms were added in shells of constant radius. The charges assigned to the atoms were $Z_{\rm Fe}=2$, $Z_{\rm S}=-1$. $V_{zz}(0\le R\le 7{\cdot}971$ Å) and $V_{zz}(0\le R\le 8{\cdot}840$ Å), which differ by the addition of a shell whose total charge is zero, were computed and found to differ by 1·6%. We therefore concluded that the calculation had converged. 232 atoms were included in the sphere.

To check the sensitivity of the computed values to the positions of the atoms, several calculations were made in which the positions of the S atoms were varied from the positions given in Table 2. The correct positions of the S atoms depend on the parameter u where u is the atomic coordinate in fractions of the cell size. u was found to be $0{\cdot}3850\pm 0{\cdot}0001$. Fig. 5 shows the effect on ΔE_Q and η of varying u.

It is evident that the value of ΔE depends on the value of u. However, the value of $eq_{\rm lat}$ for the range $0{\cdot}380\le u\le 0{\cdot}390$ lies between $0{\cdot}09\times 10^{-20}$ erg and $0{\cdot}11\times 10^{-20}$ erg. Using Burns & Wikner's (1961) value of $\gamma_\infty=-6{\cdot}17$ for Fe^{2+} we see that the crystal field contribution ($0{\cdot}55\times 10^{-20}$ erg $<\Delta E<0{\cdot}68\times 10^{-20}$ erg)

to the quadrupole splitting is insufficient to account for the splitting of $4{\cdot}6\times10^{-20}$ erg observed in pyrite.

Natural pyrite is non-stoichiometric. The measured stoichiometry ranges from $FeS_{1.93}$ to $FeS_{2.01}$. To simulate S deficiency, 2% of the S atoms were removed at random in the calculation. It was assumed that the absence of the S atoms caused no disturbance of the lattice. To maintain charge neutrality, one Fe atom for each S atom removed was given a charge of 1 rather than 2. The Fe atoms were also selected randomly. The calculation was repeated many times to find the resulting mean value of V_{zz} and its mean square deviation. The results are shown in Fig. 6. The magnitude of the calculated field is still not enough to explain the observed splitting.

It is possible for defects which result in a charge near an atom to cause a large EFG at that nucleus. A defect with a net charge of one electron at a distance of 7·4 Å from a nucleus would cause a splitting equal to that observed in pyrite. It is unlikely that this explains the spectrum of pyrite, however. If one assumes a distribution of defects such that every nucleus has at least one defect within 7·4 Å, then some nuclei are much closer to defects than others. The spread in values of the EFG due to the large variation in distances between defects and nuclei would be larger than the observed splitting. In fact, the observed line width of 0·30 mm/s can be explained as the convolution of the detector response and the minimum observable line width of the resonant transition of 0·194 mm/s (Stevens & Stevens, 1973).

Possible lattice contributions to the EFG can consist of electrostatic fields from neighboring atoms, asymmetries due to non-stoichiometry, or asymmetries due to lattice defects. We have shown that none of these are sufficient to account for the observed quadrupole splitting of pyrite.

(c) *Valence shell contributions*

We now consider the term $(1-R)q_{\rm val}$ in (4). R has been calculated for Fe^{2+} by Ingalls (1964) and found to be 0·22. $q_{\rm val}$ is given by

$$q_{\rm val}=\sum\langle 3\cos^2\theta-1\rangle\langle r^{-3}\rangle\,. \qquad (10)$$

By considering the symmetry of the wave functions the contributions from each electron in an orbital have been calculated (Bancroft, 1973).

We write (10) for p and d electrons as

$$q_{\rm val}=K_p[-N_{p_z}+\tfrac{1}{2}(N_{p_x}+N_{p_y})] \qquad (11)$$

$$q_{\rm val}=K_d[-N_{d_{z^2}}+N_{d_{x^2-y^2}}+N_{d_{xy}}-\tfrac{1}{2}(N_{d_{xz}}+N_{d_{yz}})] \qquad (12)$$

$$K_p=\tfrac{4}{5}\langle r^{-3}\rangle_p\,,\quad K_d=\tfrac{4}{7}\langle r^{-3}\rangle_d\,.$$

Since pyrite is low spin, complete localization of six electrons on the metal atom implies that $N_{d_{xy}}=N_{d_{xz}}=N_{d_{yz}}=2$, and $N_{d_{x^2-y^2}}=N_{d_{z^2}}=0$. Hence, $q_{\rm val}=0$ if the metal electrons are completely localized on the metal.

If, however, the metal electrons are delocalized by donation to a ligand, a nonzero $q_{\rm val}$ can result. Since $\langle r^{-3}\rangle_{3d}=31{\cdot}9\times10^{24}$ cm^{-3} and $\langle r^{-3}\rangle_{4p}=11{\cdot}6\times10^{24}$ cm^{-3} (Bancroft, 1973) one can see from equations (2), (11) and (12) that a slight change in the occupancy of the $3d$ or $4p$ orbitals would produce a quadrupole

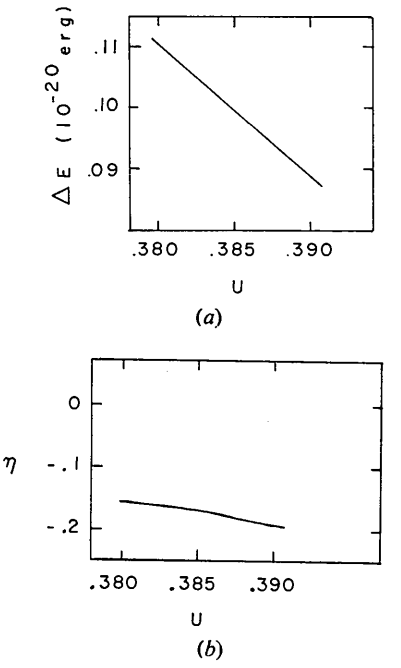

Fig. 5. Position dependence of quadrupole splitting and asymmetry parameter. (*a*) Variation of the quadrupole splitting (ΔE) as a function of the sulfur positional parameter u. (*b*) Variation of asymmetry parameter η as function of u.

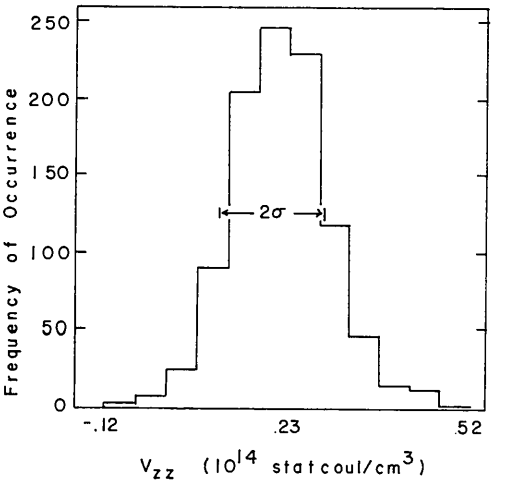

Fig. 6. Variation of EFG as a function of sulfur vacancies. The calculation of V_{zz} with S atoms removed at random was repeated 1000 times. The resulting value of V_{zz} is $0{\cdot}2124\pm0{\cdot}0948\times10^{14}$ statcoul/cm^3. This is to be compared to the value of V_{zz} for a perfect crystal, calculated to be $0{\cdot}2262\times10^{14}$ statcoul/cm^3. To find the resulting quadrupole splitting, multiply V_{zz} by $0{\cdot}449\times10^{-34}$ erg/statcoul/cm^3.

splitting of the observed magnitude. The change necessary would be

$$-N_{p_z}+\tfrac{1}{2}(N_{p_x}+N_{p_y})=0{\cdot}0923\,, \qquad (13)$$

or

$$-N_{d_{z^2}}+N_{d_{x^2-y^2}}+N_{d_{xy}}-\tfrac{1}{2}(N_{d_{xz}}+N_{d_{yz}})=0{\cdot}0336\,. \qquad (14)$$

Therefore, the results can be most readily interpreted as some delocalization of metal electrons, *i.e.* covalent bonding between Fe and S, a chemically very reasonable situation. The covalent character of Fe–S bonds has been discussed in some detail (Simon & Dahl, 1973; Averill *et al.*, 1973). The apparent lengthening of the S–S bond (Table 3) is in agreement with the band structure proposed for pyrite by Goodenough (1972) in which one of the four bonds forms an antibonding orbital with the nearest neighbor S atom and the other three orbitals form bonding orbitals with the metal orbitals.

(*d*) *Thermal shift*

In the previous section we showed that to explain the quadrupole splitting of pyrite it is necessary to consider linear combinations of Fe and S orbitals. The temperature dependence of the isomer shift provides further evidence to support this view.

The isomer shift v_s as a function of temperature and the lattice energy U is given by Josephson (1960) as

$$\frac{\partial v_s}{\partial T}=\frac{1}{2c}\frac{\partial U}{\partial T}\,. \qquad (15)$$

Kelley & King (1961) give the specific heat of a lattice containing p sublattices as

$$c_v=\tfrac{1}{3}[\tfrac{3}{2}D(\theta_D/T)+\sum^{3(p-1)}E(\theta_E/T)] \qquad (16)$$

where θ_D and θ_E are the Debye and Einstein temperatures associated with each sublattice and D and E are the Debye and Einstein functions respectively. We therefore write (16) as

$$\frac{\partial v_s}{\partial T}=\frac{\partial}{\partial T}\frac{1}{2c}[U_D(\theta_D/T)+2U_E(\theta_D/T)] \qquad (17)$$

or

$$v_s(T)-v_s(T_0)=\frac{1}{2c}[U_D(\theta_D/T)-U_D(\theta_D/T_0)+2U_E(\theta_E/T)-2U_E(\theta_E/T_0)] \qquad (18)$$

where T is the variable temperature of the absorber and T_0 is room temperature. p is taken initially to be three because pyrite has three atoms per formula unit. The values of $\theta_D=421$ K and $\theta_E=532$ K were assigned by Anderson (1937) so that the measured specific heat at high and low temperatures fitted a smooth curve of the form of (16) with $p=3$.

The isomer shift as a function of temperature is plotted in Fig. 7. It was found that to fit the data, (17) had to be changed to

$$\frac{\partial v_s}{\partial T}=\frac{1}{2c}\frac{\partial}{\partial T}[U_D(\theta_D/T)+U_E(\theta_E/T)]\,. \qquad (19)$$

The resulting curve is also plotted in Fig. 7.

This result means that below 300 K pyrite behaves as though it has two sublattices rather than the three expected. This is interpreted to mean that the S atoms are bound together by covalent bonds and move as a unit in this temperature range. The additional degrees of freedom available to the lattice as S–S vibrations or Raman modes are only excited at higher temperatures. Verble & Wallace (1969) detect no such modes between 190 and 660 cm^{-1}, or from 274 to 950 K. Eysel, Siebert & Agiogitis (1969) observe a weak Raman band at 438 cm^{-1}, with an equivalent temperature of 636 K.

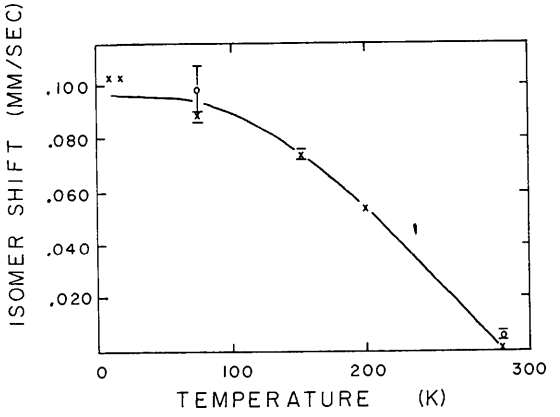

Fig. 7. Temperature dependence of the isomer shift of pyrite. The reference energy was taken to be the isomer shift of [100] pyrite relative to Fe in Cu. Both source and absorber were at room temperature (300 K).

(*e*) *Mean squared displacement*

There is considerable variation in the values of the ratios of line intensities reported previously (Table 5).

We were not able to duplicate the results of Goodman or of Garg *et al.* Notice that the intensity ratios are greatly different from 1 and that in the results of Garg *et al.* there is a large variation in the intensity ratios as a function of angle. This was not observed in any of the samples measured for this work and is also contrary to the results of Suzdalev *et al.* Goodman and Garg *et al.* do not report the source of their samples and it is therefore not possible to determine if their results are real and, if so, why such large asymmetry should be observed.

From their data Suzdalev *et al.* find that the mean squared displacement of the Fe atom is given by Table 6. Suzdalev *et al.* derive these results from the fact that the intensity ratio of the spectrum of the [110] crystal is 1·03. Likewise the asymmetry parameter η introduced in (8) is nonzero if the intensity ratio of the [100] or the [010] crystal is not equal to one.

Table 5. *Intensity ratios for oriented pyrite crystals*

Reference	Crystal orientation	A_2/A_1*
Imbert, Gerard & Wintenberger (1963)	powder	0·97
Goodman (1966)	[100]	0·86
	[100]	1·33
Garg, Lui & Puri (1974)	[100]	0·89
	[010]	0·89
	[001]	1·00 ± 0·02
	powder	1·00 ± 0·02
Suzdalev, Vinogradov & Imshennik (1972)	[100]	1·03 ± 0·01
	[110]	1·03 ± 0·01
	powder	1·03 ± 0·01
This work	[100]	1·000 ± 0·016
	[010]	1·004 ± 0·011
	[110]	1·008 ± 0·020
	powder	1·013 ± 0·031

* Intensity ratio of quadrupole pair.

Table 6. *Mean squared displacement of iron atoms in pyrite*

T (K)	$\langle x_1^2 \rangle$	$\langle x_2^2 \rangle$
90	0·81 ± 0·07	0·34 ± 0·03
300	1·22 ± 0·10	0·65 ± 0·65
600	1·88 ± 0·12	1·20 ± 0·10

$\langle x_1^2 \rangle$ parallel to [111] axis
$\langle x_2^2 \rangle$ perpendicular to [111] axis

The results of our measurements, however, give intensity ratios which are closer to one. Hence our data supports the view that the asymmetry of $\langle x^2 \rangle$ is much smaller than that reported by Suzdalev *et al.* In addition, the X-ray data shows that the asymmetry in $\langle x^2 \rangle$ cannot be as large as indicated in Table 5. The thermal parameters of the Fe atoms determined from X-ray data admit a difference between $\langle x_1^2 \rangle$ and $\langle x_2^2 \rangle$ of no more than 5 %.

A determination of the mean squared displacement of the Fe atoms using a method different from that of Suzdalev *et al.* was made using the [010] and [110] data. The method used here was to calculate the mean squared displacement in the [010] and [110] directions from recoil-free fraction measurements and then use these results to calculate the ratio of the principal axes of the thermal ellipsoid of the Fe atom.

From the results of Bykov & Hein (1962) the intensity $\varepsilon(0)$ of a Mössbauer transition at the resonance velocity $v=0$ can be written, assuming negligible absorption in the source, as

$$\varepsilon(0)=\alpha f_s[1-I_0(C_a/2)\exp(-C_a/2)] . \qquad (20)$$

Here αf_s=constants of the source, $C_a=f_a n\sigma_0 t\Gamma/2\Gamma_0$, f_a=recoil-free fraction, $n=5{\cdot}56\times10^{20}$ resonant atoms/cm^3 in pyrite, $\sigma_0=2{\cdot}355\times10^{-18}$ cm^2 resonant cross section of ^{57}Fe, $\Gamma_0=0{\cdot}19$ mm/s minimum observable linewidth of ^{57}Fe, $\Gamma=0{\cdot}30$ mm/s observed linewidth of pyrite, t=thickness of sample, I_0=first order Bessel function of imaginary argument.

From the observed spectrum we measure the resonance intensity $I(0)$ and the background intensity $I(\infty)$. Then

$$\varepsilon(0)/\alpha f_s=[I(\infty)-I(0)]/I(\infty)\equiv R .$$

Equation (20) may be rearranged as

$$I_0(x)=(1-R)\exp(x) . \qquad (21)$$

Here $x=C_a/2$. Solving this equation for x, given the observed values of R, we can then use the definition of C_a and the recoil-free fraction to write

$$f_a=\exp(-k^2\langle x^2\rangle)=\exp(-4\pi^2\langle x^2\rangle/\lambda^2)$$

$$\langle x^2\rangle=-(\lambda^2/4\pi^2)\ln f_a=-(\lambda^2/4\pi^2)\ln(4\Gamma_0 x/n\sigma\Gamma t) . \qquad (22)$$

Fig. 8 shows the temperature dependence of $\langle x^2 \rangle$ calculated in this way. The close agreement between the component of $\langle x^2 \rangle$ in the [010] direction and the component of $\langle x^2 \rangle$ in the [110] direction indicates that $\langle x^2 \rangle$ has very little angular dependence.

We now calculate the degree of angular dependence. We assume that $\langle x^2 \rangle$ may be described as an ellipsoid whose defining equation is the following special case of the general equation:

$$ax^2+ay^2+bz^2=1 . \qquad (23)$$

The components of $\langle x^2 \rangle$ are $\langle x_1^2 \rangle=1/\sqrt{b}$ and $\langle x_2^2 \rangle=1/\sqrt{a}$. We now use the transformation of axes given in equation (9) to ensure that the major axis of the ellipsoid is directed along the [111] axis as required by symmetry.

Computing the projection of the ellipsoid along the [110] and [010] directions, we may then use the measured values of $\langle x^2 \rangle$ in those directions to find the ratio $\langle x_2^2 \rangle/\langle x_1^2 \rangle=1{\cdot}089\pm0{\cdot}066$. We conclude therefore that the difference between $\langle x_1^2 \rangle$ and $\langle x_2^2 \rangle$ can be no greater than 9 %.

References

ANDERSON, C. T. (1937). *J. Amer. Chem. Soc.* **59**, 486–487.

AVERILL, B. A., HERSKOVITZ, T., HOLM, R. H. & IBERS, J. A. (1973). *J. Amer. Chem. Soc.* **95**, 3523–3532.

BALCH, A. L. (1969). *J. Amer. Chem. Soc.* **91**, 6962–6967.

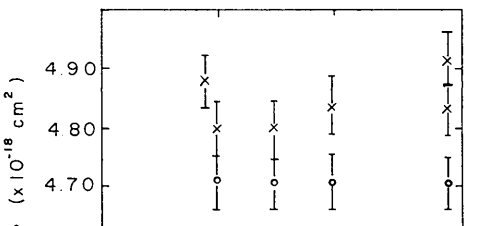

Fig. 8. Temperature dependence of $\langle x^2 \rangle$. The mean squared displacement was calculated from measurements of the recoil-free fraction as described in the text. Crosses denote [010] measurements. Open circles denote [110] measurements.

BANCROFT, G. M. (1973). *Mössbauer Spectroscopy: An Introduction for Chemists and Geochemists*. New York: Wiley.

BERNAL, I., DAVIS, R. B., GOOD, M. L. & CHANDRA, S. (1972). *J. Coord. Chem.* **2**, 61–65.

BROSTIGEN, G. & KJEKSHUS, A. (1969). *Acta Chem. Scand.* **23**, 2186–2188.

BURNS, G. & WIKNER, E. G. (1961). *Phys. Rev.* **121**, 155–158.

BUSING, W. R. & LEVY, H. A. (1967). *Acta Cryst.* **22**, 457–464.

BUSING, W. R., MARTIN, K. O. & LEVY, H. A. (1962). *ORFLS*. Oak Ridge National Laboratory Report ORNL-TM-305.

BYKOV, G. A. & HEIN, P. Z. (1962). *J. Exp. Theor. Phys. (USSR)*, **43**, 909–918; translated in *Sov. Phys. JETP.* (1963). **16**, 646–651.

CHRISMAN, B. L. & TUMOLILLO, T. A. (1969). *Computer Analysis of Mössbauer Spectra*, Tech. Rep. No. 178, Department of Physics, Univ. of Illinois, Urbana, Illinois.

COGSWELL, G. W. (1975). Private communication.

CROMER, D. T. (1965). *Acta Cryst.* **18**, 17–23.

CROMER, D. T. & WABER, J. T. (1965). *Acta Cryst.* **18**, 104–109.

EPSTEIN, L. M. & STRAUB, D. K. (1969). *Inorg. Chem.* **8**, 784–789.

EYSEL, H. H., SIEBERT, H. & AGIORGITIS, G. (1969). *Z. Naturforsch. (B)*, **24**, 932–933.

FRANK, E. & ABELEDO, C. R. (1966). *Inorg. Chem.* **5**, 1453–1455.

FURNAS, T. C. (1957). *Single Crystal Orienter Instruction Manual*, General Electric Co., Milwaukee, WI.

GARG, V. K., LUI, Y. S. & PURI, S. P. (1974). *J. Appl. Phys.* **45**, 70–72.

GASH, A. G., RODESILER, P. F. & AMMA, E. L. (1974). *Inorg. Chem.* **13**, 2429–2434.

GOLDANSKII, V. I. & HERBER, R. H. (1968). Editors, *Chemical Applications of Mössbauer Spectroscopy*. New York: Academic Press.

GOLDING, R. M. & WHITFIELD, H. J. (1966). *Trans. Faraday Soc.* **62**, 1713–1716.

GOODENOUGH, J. B. (1972). *J. Solid State Chem.* **5**, 144–152.

GOODMAN, R. H. (1966). *Chem. Canad.* **18**, 31–36; *Chem. Abs.* **65**, 4683d.

HAMILTON, W. C. (1964). Program *GONO*-9, Brookhaven National Laboratory, with local modifications.

IMBERT, P., GERARD, A. & WINTENBERGER, M. (1963). *C. R. Acad. Sci. Paris*, **256**, 4391–4393.

INGALLS, R. (1964). *Phys. Rev.* **133**, A787–A795.

JOHNSON, C. K. (1965). *ORTEP*, second revision. Oak Ridge National Laboratory Report ORNL-3794.

JOSEPHSON, B. D. (1960). *Phys. Rev. Lett.* **4**, 341.

KELLEY, K. K. & KING, E. G. (1961). *Entropies of Inorganic Compounds*; *Selected Values of Thermal Properties of Metals and Alloys*. U.S. Bureau of Mines Bulletin No. 592, p. 5.

KNOX, K. (1967). *Master Card Program for Picker Four-Angle Programmer*. Picker Instruments, Cleveland, OH.

LEVY, H. A. (1956). *Acta Cryst.* **9**, 679.

MERRITHEW, P. B. & RASMUSSEN, P. G. (1972). *Inorg. Chem.* **11**, 325–330.

PARKER, H. M. & WHITEHOUSE, W. J. (1932). *Phil. Mag. Ser.* 7, **14**, 939–961.

RICHARDS, R., JOHNSON, C. E. & HILL, H. A. O. (1968). *J. Chem. Phys.* **48**, 5231–5238.

RODESILER, P. F. & AMMA, E. L. (1971). *Acta Cryst.* B**27**, 1687–1692.

SERRES, A. (1953). *J. Phys. Radium*, **14**, 689–690.

SIMON, G. L. & DAHL, L. F. (1973). *J. Amer. Chem. Soc.* **95**, 2164–2174.

SMITH, F. G. (1942). *J. Min. Soc. Amer.* **27**, 1–19.

SMITH, J. M. (1975). *Scientific Analysis on the Pocket Calculator*, p. 271. New York: Wiley.

STERNHEIMER, R. & FOLEY, H. M. (1956). *Phys. Rev.* **102**, 731–732.

STEVENS, J. G. & STEVENS, V. E. (1973). Editors, *Mössbauer Effect Data Index*. New York: IFI/Plenum.

SUZDALEV, I. P., VINOGRADOV, I. A. & IMSHENNIK, V. K. (1972). *Sov. Phys. Solid State*, **14**, 1136–1142.

VAINSTEIN, E. E., VALOV, P. M., LARIMOV, S. L. & SHULLMAN, V. M. (1966). *Dokl. Akad. Nauk SSSR*, **168**, 130.

VERBLE, J. L. & WALLACE, R. F. (1969). *Phys. Rev.* **182**, 783–789.

YOUNG, R. A. (1965). *Trans. Amer. Cryst. Assoc.* **1**, 42–66.